Heterocyclic quinol-type fluorophores. Part 2. Solid-state fluorescence enhancement behaviour of benzofurano[3,2-*b*]-naphthoquinol-type † clathrate hosts upon inclusion of amine molecules ‡

Katsuhira Yoshida,* Yousuke Ooyama, Sachiko Tanikawa and Shigeru Watanabe

Department of Material Science, Faculty of Science, Kochi University, Akebono-cho, Kochi 780-8520, Japan

Received (in Cambridge, UK) 9th October 2001, Accepted 11th January 2002
First published as an Advance Article on the web 12th February 2002

Novel benzofuranonaphthoquinol-type clathrate hosts, which exhibit fluorescence enhancement behaviour with a blue shift of the emission maximum upon formation of clathrates with amines, have been developed. The clathrate compounds are formed not only by cocrystallization from amine solutions but also by solid (host)–gas (amine vapour) contact. The time-dependent fluorescence excitation and emission spectral changes upon exposure to various amine vapours were measured for crystals and thin films of the host compound. The time-scale for the spectral changes has been greatly shortened by using thin films instead of crystals. The crystal structures of the clathrate compounds have been determined by X-ray analysis. On the basis of the spectral data and the crystal structures, the effects of the enclathrated guest on the solid-state photophysical properties of the clathrate compounds are discussed.

Introduction

Chromogenic receptors which give spectroscopic signals in response to recognition of ions or molecules are the subject of current research interests, owing to their fundamental photophysical properties and their wide range of potential applications in analytical and material sciences.[1] Clathrate formation by solid–gas contact has been used to design chemical sensor materials for neutral molecules.[2] Other studies have applied clathrate formation to a fluorescence sensing system for the detection of organic solvent molecules.[3] The novel solvoluminescent behaviour exhibited by crystalline gold metallacycles reacting with solvent vapours has recently been reported.[4] However, there are still very few clathrate hosts that can exhibit sensitive fluorescence changes upon inclusion of organic guest molecules.

Recently, we have developed novel fluorescent clathrate hosts that can form crystalline inclusion compounds with organic solvent molecules.[5–7] The solid-state fluorescence of the clathrate hosts was enhanced to various degrees depending on the enclathrated solvent molecules. Such fluorescence spectral changes are of great interest from the point of developing new chemosensors based on clathrate formation. In addition, the effects of enclathrated solvent molecules on the molecular packing structure and on the solid-state photophysical properties in the crystalline state are also very interesting. In the preceding paper,[8] we have reported the absorption and fluorescence characteristics of the isomeric benzofurano[3,2-*b*]naphthoquinols **2a**–**2c** and **3a**–**3c** in solution and in the crystalline state. In this paper, we report the amine-inclusion ability and concomitant fluorescence enhancement behaviour of the quinols in the crystalline state and in thin films. The changes in the solid-state absorption and fluorescence properties and the X-ray crystal structures of the host compounds upon formation of the clathrate compounds have been elucidated. The relationship between the observed solid-state photophysical properties and the X-ray crystal structures is discussed on the basis of the spectral data and the crystal structures.

Results and discussion

Inclusion ability in the crystalline state

Specific structural units such as a rigid backbone, bulky substituents, and anchor groups are required for the design of clathrate host molecules.[9] In order to create new clathrate hosts having fluorescence emission ability, we employed a benzofurano[3,2-*b*]naphthoquinol fluorophore as a rigid backbone with anchor groups. Thus, we have designed and synthesized 3-(dibutylamino)benzofurano[3,2-*b*]naphthoquinol derivatives **2a**–**2c** and **3a**–**3c** from compound **1**.[8] In order to investigate their inclusion ability, we recrystallized the quinol compounds from various organic solvents such as ethanol, acetonitrile, benzene, 1,4-dioxane and morpholine. The quinols **2a**, **2b**, **3a**, and **3b** did not form any inclusion compounds. However, we have found that the quinols **2c** and **3c** yield inclusion compounds in stoichiometric ratios with amines. These results suggest that the phenyl group of **2c** and **3c** works effectively as a rigid block to provide cavities for accommodation of guest molecules in the crystal. We could not investigate the inclusion ability of **2c** for different amine solvents, because the yield of **2c** was quite low compared to that of **3c** as reported in the preceding paper.[8] Therefore, host **3c** was mainly used in this study. The characteristics of the guest-free and amine-inclusion crystals are summarized in Table 1. The guest-free crystals were obtained by recrystallization of **2c** from 99% ethanol and of **3c** from a mixture of chloroform–*n*-hexane, respectively. For preparation of the clathrate crystals, the respective amine or amine-containing solvents were used. All the amine-inclusion crystals exhibit a blue shift in colour and stronger fluorescence intensity compared to their respective guest-free crystals.

† The IUPAC name for the parent benzofurano[3,2-*b*]naphthoquinone is naphtho[2,3-*b*]benzofuran-6,11-dione.

‡ Electronic supplementary information (ESI) available: Table S1 containing crystal data and structure refinement parameters for amine-inclusion compounds of **2c** and **3c**. See http://www.rsc.org/suppdata/p2/b1/b109202m/

 DOI: 10.1039/b109202m

Table 1 Host : guest ratios, crystal form, and colour of the guest-free and amine-inclusion crystals of **2c** and **3c**

Host	Guest	Host : guest (mole ratio)	Crystal form	Crystal colour	Recrystallization solvent
2c	None	1 : 0	Prism	Orange	99% Ethanol
	Piperidine	1 : 1	Needle	Yellow	Piperidine–water (1 : 1)
	Morpholine	1 : 1	Needle	Yellowish orange	Morpholine–water (1 : 1)
3c	None	1 : 0	Prism	Yellowish orange	Chloroform–*n*-hexane (1 : 1)
	Diethylamine	1 : 1	Needle	Yellow	Diethylamine–water (1 : 1)
	Piperazine	2 : 1	Prism	Yellow	Piperazine–99% ethanol
	Morpholine	1 : 1	Needle	Yellow	Morpholine
	Piperidine	1 : 1	Prism	Light yellow	Piperidine

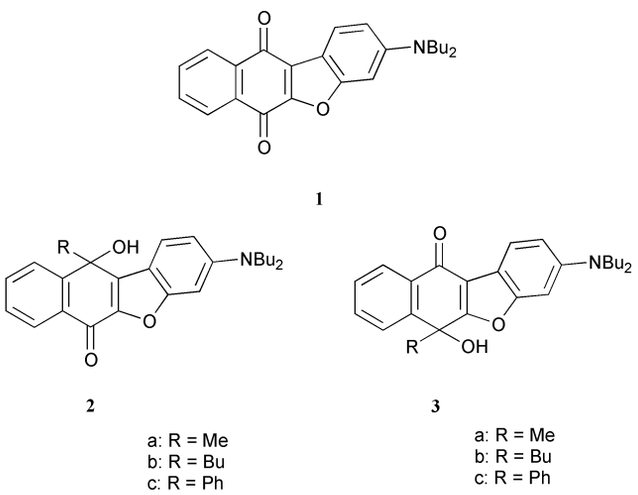

Solid-state fluorescence properties of the clathrate compounds

In order to investigate the influence of clathrate formation on the solid-state absorption and fluorescence properties of each host compound, the fluorescence excitation and emission spectra of the guest-free and the amine-inclusion crystals of **2c** and **3c** were measured. The spectra recorded at the corresponding emission or excitation maxima of the guest-free and the amine-inclusion crystals are shown in Figs. 1 and 2. Some

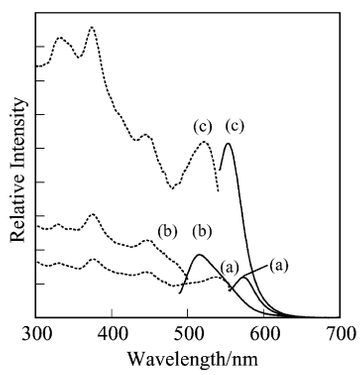

Fig. 1 Excitation (· · ·) and emission (—) spectra of the guest-free and amine-inclusion crystals of **2c**: (a) **2c** (guest-free), λ_{ex} = 537, λ_{em} = 574 nm; (b) **2c**–piperidine (1 : 1), λ_{ex} = 469, λ_{em} = 517 nm; (c) **2c**–morpholine (1 : 1), λ_{ex} = 522, λ_{em} = 533 nm.

differences in the spectral changes are observed between the two isomers. The size of the blue shift of the excitation and emission maxima and the increase in the fluorescence intensity are greatly dependent on the enclathrated amine molecules.

In the case of **2c**, the 537 nm band observed in the excitation spectrum of the guest-free crystals shifts to 522 and *ca.* 469 nm in those of the morpholine- and piperidine-inclusion crystals, respectively (Fig. 1). The guest-free crystal exhibits relatively weak fluorescence with an emission maximum at 574 nm, while the morpholine- and piperidine-inclusion crystals exhibit stronger fluorescence intensity with blue-shifted emission

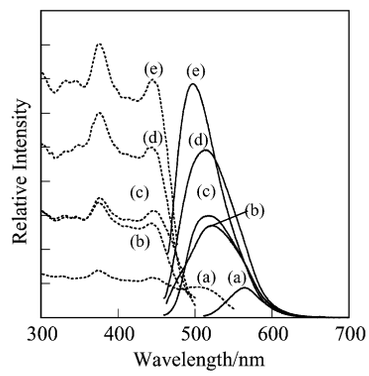

Fig. 2 Excitation (· · ·) and emission (—) spectra of the guest-free and amine-inclusion crystals of **3c**: (a) **3c** (guest-free), λ_{ex} = 504, λ_{em} = 569 nm; (b) **3c**–piperazine (2 : 1), λ_{ex} = 438, λ_{em} = 519 nm; (c) **3c**–diethylamine (1 : 1), λ_{ex} = 447, λ_{em} = 518 nm; (d) **3c**–morpholine (1 : 1), λ_{ex} = 446, λ_{em} = 507 nm; (e) **3c**–piperidine (1 : 1), λ_{ex} = 444, λ_{em} = 501 nm.

maxima at 533 and 517 nm, respectively. The degree of fluorescence enhancement of **2c**–morpholine (1 : 1) is considerably bigger than that of **2c**–piperidine (1 : 1).

In contrast, in the case of **3c**, the 504 nm band observed in the excitation spectrum of the guest-free crystal shifts to 447, 438, 446, and 444 nm in those of the diethylamine-, piperazine-, morpholine- and piperidine-inclusion crystals, respectively (Fig. 2). The solid-state fluorescence spectrum is also dramatically changed depending on the nature of the enclathrated amine molecules. The guest-free crystal exhibits a weak fluorescence band with an emission maximum at 569 nm, whereas the amine-inclusion crystals exhibit a stronger fluorescence band with a blue-shifted emission maximum. The fluorescence enhancement increases in the following order: **3c** (guest-free): λ_{em} = 569 nm < **3c**–piperazine (2 : 1): λ_{em} = 519 nm < **3c**–diethylamine (1 : 1): λ_{em} = 518 nm < **3c**–morpholine (1 : 1): λ_{em} = 508 nm < **3c**–piperidine (1 : 1): λ_{em} = 501 nm. The fluorescence maximum shifts to shorter wavelength with an increase in the fluorescence intensity in this case.

Fluorescence sensing behaviour of the guest-free crystals and thin films

The corresponding inclusion compounds were also formed and similar fluorescence enhancement was observed when the guest-free crystals or thin films of **3c** were placed in a vessel saturated with amine vapour at room temperature.

As an example, Fig. 3 shows the time-dependent spectral changes that occurred when the guest-free crystals of **3c** were placed in a vessel saturated with piperidine vapour at 30 °C. The initial excitation band at 504 nm gradually disappears and the fluorescence band at 569 nm shifts to shorter wavelength with an increase in fluorescence intensity. It took about 18–20 h to reach the final saturated excitation and emission spectra which are in good agreement with the spectra of crystals of the corresponding clathrate compound (**3c**–piperidine, 1 : 1).

In contrast, as shown in Fig. 4(a) and 4(b), when a thin film of **3c** was used instead of the guest-free crystals, the spectral

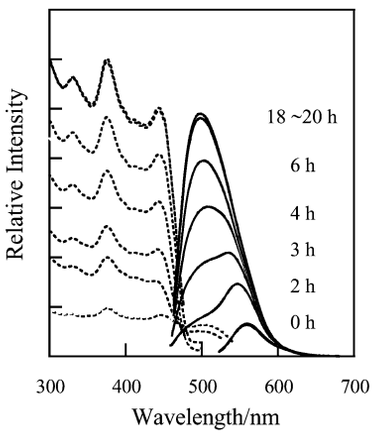

Fig. 3 Time-dependent spectral changes of the guest-free crystals of **3c** upon exposure to piperidine vapour at 30 °C; the excitation (···) and emission (—) spectra were recorded at their corresponding emission and excitation maxima.

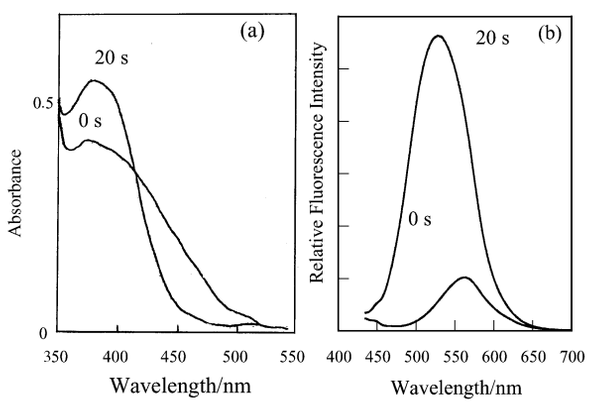

Fig. 4 (a) Absorption and (b) fluorescence spectral changes of a thin film of **3c** upon exposure to piperidine vapour at 30 °C.

changes were complete within 20 s. A decrease in the absorbance of a shoulder around 420–500 nm and an increase in the absorbance of a band at around 376 nm are observed with an isosbestic point at 415 nm. The corresponding fluorescence spectra show a dramatic increase in fluorescence intensity with a blue shift of the emission maximum from 560 to 533 nm. When other amines were used instead of piperidine, similar absorption and fluorescence spectral changes were also observed and were almost saturated within 10–20 s. These results indicate that the time-scale for the spectral changes can be greatly shortened by using thin films instead of crystals. Fig. 5 summarizes the results of the fluorescence spectral

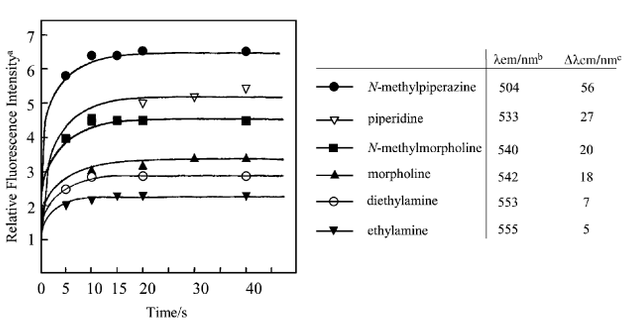

Fig. 5 Time-dependent fluorescence spectral changes of thin films of **3c** upon exposure to various amine vapours at 30 °C; [a] RFI = FI (after exposure)/FI (before exposure), [b] λ_{ex} = 376 nm, [c] $\Delta\lambda_{em}$ = [560 (before exposure) − λ_{em} (after exposure)] nm.

changes of thin films of **3c** upon exposure to various gaseous amines. The degrees of fluorescence enhancement and the blue shift of the fluorescence wavelength are dependent on the identity of the enclathrated amine molecule and increase in the following order: ethylamine < diethylamine < morpholine < *N*-methylmorpholine < piperidine < *N*-methylpiperazine. The formation of clathrates (**3c**–guest, 1 : 1) was indicated for all of the above amines from the ^{1}H NMR integrations of the dissolved samples prepared from the exposed thin films. Both the fluorescence enhancement and the blue shift values of the thin films are not as large as those of the crystals. Although there are some differences in the spectral changes between the thin film and the crystalline state, the above results suggest that the mechanism of fluorescence sensing is substantially the same in both cases. The existence of a somewhat amorphous structure in the films may cause there to be fewer spectral changes for the thin films compared to the guest-free crystals.

Crystal structures of the amine-inclusion compounds

As shown in the previous sections, the solid-state fluorescence properties of **2c** and **3c** are considerably changed by clathrate formation with various amines. The guest-free crystals of **2c** and **3c** exhibit relatively weak fluorescence, whereas the amine-inclusion crystals exhibit stronger fluorescence with a blue-shifted emission maximum. The crystal structures of the guest-free crystals of **2c** and **3c** have already been determined by X-ray diffraction and are reported in the preceding paper.[8] The packing structures demonstrate that the crystals of the two isomers are built up from a centrosymmetric dimer unit which is composed of a pair of the host enantiomers bound cofacially by two intermolecular hydrogen bonds; the schematic structures are shown in Fig. 6. We have proposed that the close

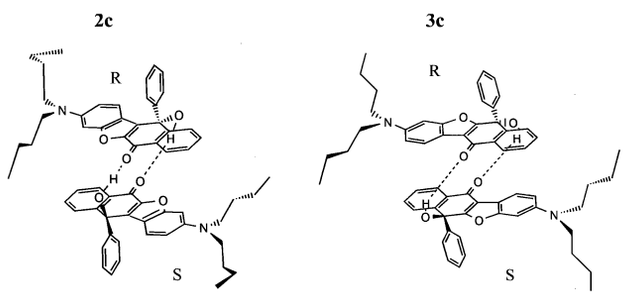

Fig. 6 Schematic structure of a pair of the host enantiomers for the guest-free crystals of **2c** and **3c**. Hydrogen bonds are shown as dotted lines.

π–π overlap of the host enantiomers causes π–π interactions, leading to the red shift of the absorption and fluorescence wavelength maxima and the strong fluorescence quenching of **2c** and **3c** in the crystalline state.[8] The effects of intermolecular π–π interactions of chromophores with intramolecular charge transfer character on the solid-state photophysical properties, such as red-shift of absorption [10–12] or fluorescence quenching,[13] have been reported previously. Mizuguchi investigated the correlation between the absorption spectra and the X-ray crystal structures of some DPP pigments on the basis of exciton coupling effects.[14]

In order to investigate the effects of the enclathrated guest on the fluorescence properties of the crystals, we have further determined the crystal structures of the morpholine- and piperidine-inclusion compounds of **2c** and **3c**. The crystal systems of the four clathrate compounds are monoclinic (for **2c**–morpholine) and triclinic (for **2c**–piperidine, **3c**–morpholine, and **3c**–piperidine), respectively. The space group of **2c**–morpholine is *C*2/*c* and that of the other three clathrate crystals is $P\bar{1}$, respectively. Figs. 7 and 8 show (a) a stereoview of the molecular packing structure, (b) a schematic structure, (c)

a side view, and (d) a top view of a cluster unit of the crystals of **2c**–morpholine and **2c**–piperidine, respectively. The packing structures demonstrate that both crystals are built up from a centrosymmetric cluster unit, and that the molecules are arranged in a "herringbone" fashion in **2c**–morpholine and as "bricks in a wall" in **2c**–piperidine, respectively. The cluster unit

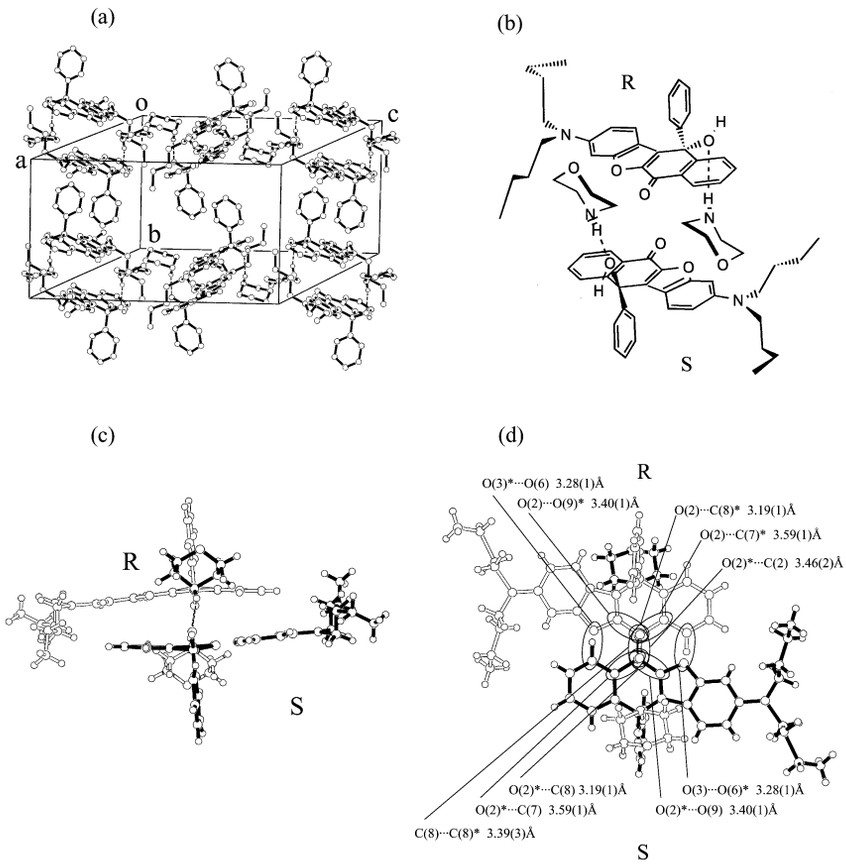

Fig. 7 Crystal packing and hydrogen bonding pattern of **2c**–morpholine: (a) a stereoview of the molecular packing structure, and (b) a schematic structure, (c) a side view, and (d) a top view of a cluster unit.

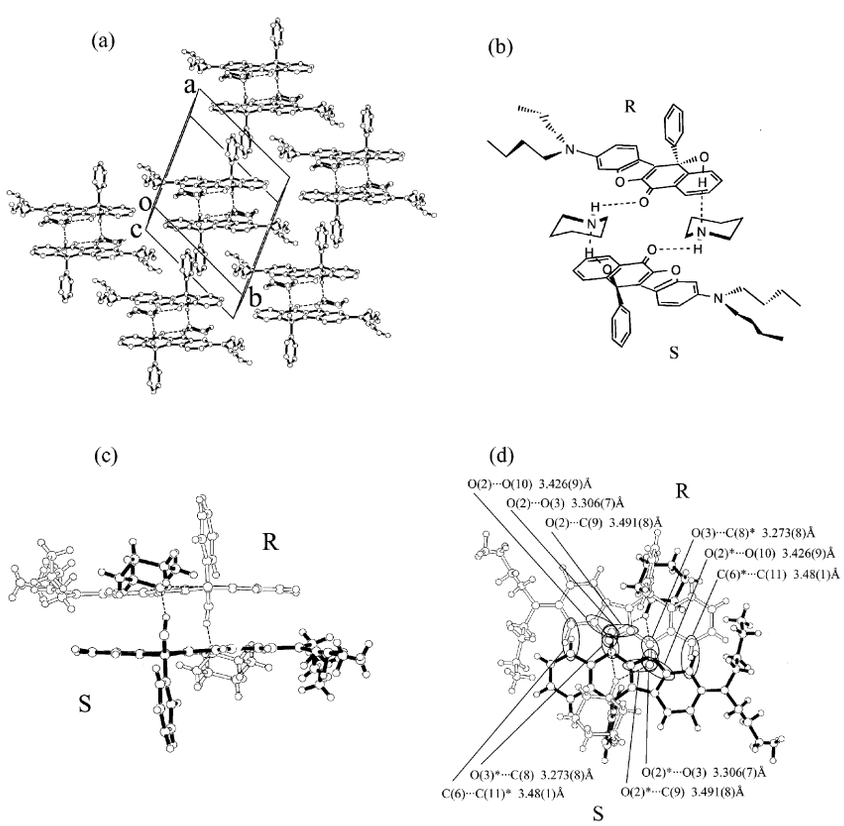

Fig. 8 Crystal packing and hydrogen bonding pattern of **2c**–piperidine: (a) a stereoview of the molecular packing structure, and (b) a schematic structure, (c) a side view, and (d) a top view of a cluster unit.

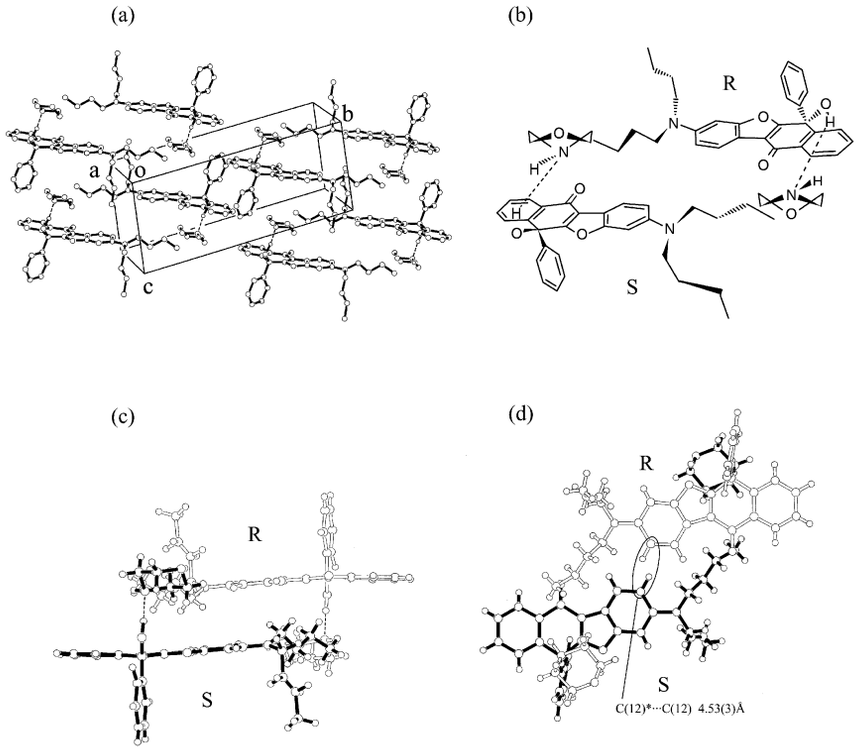

Fig. 9 Crystal packing and hydrogen bonding pattern of **3c**–morpholine: (a) a stereoview of the molecular packing structure, and (b) a schematic structure, (c) a side view, and (d) a top view of a cluster unit.

of the two crystals is composed of four molecules: a pair of enantiomers of the host **2c** and two guest molecules [Fig. 7(b) and 8(b)]. There is no observed intermolecular hydrogen bond between the host molecules in both crystals. Instead, the formation of intermolecular hydrogen bonds occurs between the host and guest molecules to yield the centrosymmetric hydrogen-bonded cluster unit. The π–π overlap between the host enantiomers in the cluster is shown in Fig. 7(d) and 8(d), where the top view of the pair of enantiomers is drawn together with non-bonded interatomic π–π contacts of less than 3.6 Å. There are 10 (= 5 × 2) short interatomic π–π contacts in the cluster unit, and no hydrogen bonding interactions and no short π–π contacts of less than 3.6 Å are observed between neighboring clusters in both crystals. Since the guest-free crystal of **2c** has 18 (= 9 × 2) short non-bonded interatomic π–π contacts of less than 3.6 Å in the pair of enantiomers,[8] we confirm that the enclathrated amine molecules considerably weaken the host–host π–π interactions. In addition, there is a difference in the π–π overlap range between **2c**–morpholine and **2c**–piperidine: the overlap extends over the whole edge of the heterocyclic quinol ring in the latter compound, while the range of the overlap narrows in the former compound. The difference in the π–π overlap in the crystals of the guest-free, **2c**–morpholine, and **2c**–piperidine compounds seems to be well reflected in their solid-state fluorescence intensities as the fluorescence intensity increases with a decrease in the host–host π–π interactions (see Fig. 1). However, a good correlation could not be drawn for the blue-shift values of the fluorescence excitation and emission wavelength maxima. The differences in the intermolecular hydrogen bonding and molecular packing modes must also be intricately related to the blue shift of the absorption and fluorescence wavelengths.

By way of comparison, the crystal packing and hydrogen bonding patterns of **3c**–morpholine and **3c**–piperidine are shown in Figs. 9 and 10. There is also no observed intermolecular hydrogen bond between the host molecules in these amine-inclusion crystals. The packing structures demonstrate that a centrosymmetric cluster unit is the building unit of the crystals, and that the molecules are arranged in a "bricks in a wall" fashion in both crystals. The cluster unit is composed of four molecules: a pair of enantiomers of the host and two guest molecules. Intermolecular hydrogen bonds between the host and guest molecules in the cluster are observed in **3c**–morpholine, while no such hydrogen bonds are observed in **3c**–piperidine as shown in the schematic structures in Figs. 9(b) and 10(b), respectively. Furthermore, as shown in the top views of the pairs of enantiomers in **3c**–morpholine and in **3c**–piperidine, there are no short non-bonded π–π contacts of less than 3.6 Å [Fig. 9(d) and 10(d)]. The shortest non-bonded interatomic distance between the pairs of enantiomers is 4.53(3) Å for **3c**–morpholine and 4.85(2) Å for **3c**–piperidine, respectively. Since there are 8 (= 4 × 2) short non-bonded interatomic π–π contacts in the guest-free crystal of **3c**,[8] a comparison of the above three crystal structures confirms that the strength of the π–π interactions decreases in the following order: **3c** (guest-free) > **3c**–morpholine > **3c**–piperidine. As seen in Fig. 2, the solid-state fluorescence intensity for the three crystals increases in the reverse order, indicating that the destruction of the host–host π–π interactions by the enclathrated amine molecules is the cause of the guest-dependent fluorescence enhancement behaviour.

Summary and conclusions

The solid-state photophysical properties of the guest-free and amine-inclusion clathrate compounds of the benzofurano-naphthoquinol-type fluorescent hosts have been investigated. A dramatic fluorescence enhancement and a blue-shift of the absorption and fluorescence wavelength maxima are observed, depending on the nature of the enclathrated amine molecules. A comparison of the X-ray crystal structures of the guest-free and clathrate compounds indicates that the enclathrated guest molecules break the intermolecular hydrogen bonds binding a pair of host enantiomers and enlarge the distance between the host–host aromatic planes. It is confirmed from the spectral data and the X-ray crystal structures that the destruction

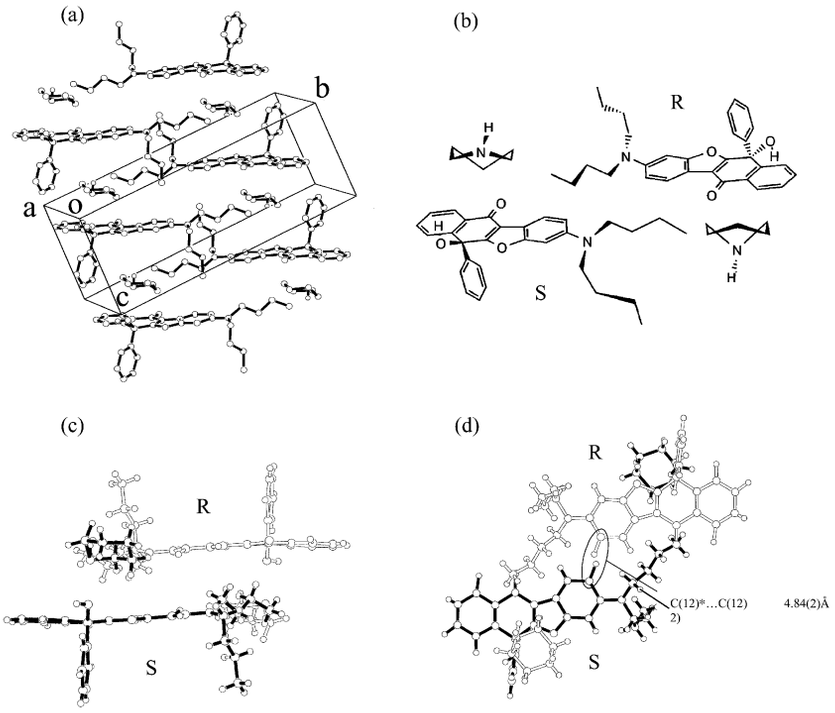

Fig. 10 Crystal packing and hydrogen bonding pattern of **3c**–piperidine: (a) a stereoview of the molecular packing structure, and (b) a schematic structure, (c) a side view, and (d) a top view of a cluster unit.

of the host–host π–π interactions by the enclathrated amine molecules is the main reason for the guest-dependent fluorescence enhancement behaviour. We believe that these results are useful for the development of new solid chemosensors and for the improvement of pigmentary solid-state fluorescence.

Experimental

Absorption spectra were measured with a Ubest-30 spectrophotometer. Fluorescence emission and excitation spectra were measured with a JASCO FP-777 spectrophotometer. Elemental analyses were recorded on a Perkin Elmer 2400 II CHN analyzer. ^{1}H NMR spectra were recorded on a JNM-LA400 (400 MHz) FT NMR spectrometer with tetramethylsilane (TMS) as an internal standard. Single-crystal X-ray diffraction was performed on a Rigaku AFC7S diffractometer.

Preparation of thin films

Thin films of **3c** were prepared on glass plates by a conventional vacuum-vapour deposition method using vacuum evaporation equipment (Sinkukiko VPC-260 F). The films of 200 ± 10 μm thickness, measured with a surface profilometer (Sloan Technology Dektak 3-ST), were used for checking the spectral changes by contact with amine vapours.

Measurement of the time-dependent spectral changes

The guest-free crystals or thin films of the host quinols were placed in a vessel saturated with amine vapour at 30 °C. The exposed samples were taken out at different time intervals, and the measurement of the absorption and fluorescence spectra was carried out. For the measurement of the solid-state fluorescence excitation and emission spectra of the crystals, a JASCO FP-1060 attachment was used.

In the case of the thin films, the glass plate of the exposed film was fixed to the cell holder of the absorption or the fluorescence spectrophotometer. The host : guest ratios of the exposed samples were determined by means of ^{1}H NMR integration.

Preparation of amine-inclusion crystals of 2c and 3c

The corresponding host compound was dissolved with heating in a solvent containing the respective amine, as shown in Table 1. The solution was filtered and kept for a few days at room temperature. The crystals that formed were collected by filtration. The host : guest stoichiometric ratio of the inclusion compounds was determined by means of ^{1}H NMR integration and CHN analysis.

X-Ray crystal structure determinations

The reflection data were collected at 23 ± 1 °C on a Rigaku AFC7S four-circle diffractometer with graphite-monochromated Mo-Kα (λ = 0.71069 Å) radiation at 50 kV and 30 mA. The crystal data and details of parameters associated with data collection for the amine-inclusion compounds are given in Table S1. The reflection intensities were monitored by three standard reflections for every 150 reflections. An empirical absorption correction based on azimuthal scans of several reflections was applied. The transmission factors ranged from 0.92 to 1.00 for **2c**–morpholine, from 0.96 to 1.00 for **2c**–piperidine, from 0.97 to 1.00 for **3c**–morpholine, and from 0.93 to 1.00 for **3c**–piperidine, respectively. The data were corrected for Lorentz and polarization effects. A correction for secondary extinction was applied. The crystal structure of **3c**–morpholine was solved by direct methods using SAPI 91[15] and the crystal structures of **2c**–morpholine, **2c**–piperidine, and **3c**–piperidine were solved by direct methods using SIR92,[16] respectively. The structures were expanded using Fourier techniques.[17] The non-hydrogen atoms were refined anisotropically. Some hydrogen atoms were refined isotropically, the rests were fixed geometrically and not refined. All calculations were performed using the teXsan[18] crystallographic software package of Molecular Structure Corporation. CCDC reference numbers 172464–172467. See http://www.rsc.org/

suppdata/p2/b1/b109202m/ for crystallographic files in .cif or other electronic format or Table S1.

Acknowledgements

The present work was partly supported by the Grant-in-Aid for Exploratory Research (No. 09875223) from the Ministry of Education, Science, Sports, and Culture, and also supported by the Tokyo Ohka Foundation for the Promotion of Science and Technology.

References

1 *Fluorescent Chemosensors for Ions and Molecule Recognition, ACS Symposium Series No. 538*, ed by A. W. Czarnik, American Chemical Society, Washington, DC, 1992; A. P. de Silva, H. Q. N. Gunaratne, T. Gunnlaugsson, A. J. M. Huxley, C. P. McCoy, J. T. Rademacher and T. E. Rice, *Chem. Rev.*, 1997, **97**, 1515.
2 K. Buhlmann, J. Reinbold, K. Cammann, K. Skobridis, A. Wierig and E. Weber, *J. Anal. Chem.*, 1994, **348**, 549; J. Reinbold, K. Buhlmann, K. Cammann, A. Wierig, C. Wimmer and E. Weber, *Sens. Actuators, B*, 1994, **18–19**, 77.
3 T. H. Brehmer, P. P. Korkas and E. Weber, *Sens. Actuators, B*, 1997, **44**, 595; E. Weber, T. Hens, Q. Li and T. C. W. Mark, *Eur. J. Org. Chem.*, 1999, 1115.
4 E. Y. Fung, M. M. Olmstead, J. C. Vickery and A. L. Balch, *Coord. Chem. Rev.*, 1998, **171**, 151; M. M. Olmstead, F. Jiang, S. Attar and A. L. Balch, *J. Am. Chem. Soc.*, 2001, **123**, 3260.
5 K. Yoshida, J. Yamasaki, Y. Tagashira, H. Miyazaki and S. Watanabe, *Chem. Lett.*, 1996, 9; K. Yoshida, T. Tachikawa, J. Yamasaki, S. Watanabe and S. Tokita, *Chem. Lett.*, 1996, 1027.
6 (*a*) K. Yoshida, H. Miyazaki, Y. Miura, Y. Ooyama and S. Watanabe, *Chem. Lett.*, 1999, 837; (*b*) K. Yoshida, Y. Ooyama, S. Tanikawa and S. Watanabe, *Chem. Lett.*, 2000, 714.
7 K. Yoshida, K. Uwada, H. Kumaoka, L. Bu and S. Watanabe, *Chem. Lett.*, 2001, 808.
8 Part 1, preceding paper: K. Yoshida, Y. Ooyama, H. Miyazaki and S. Watanabe, *J. Chem. Soc., Perkin Trans. 2*, 2002 (DOI: 10.1039/b109198k).
9 E. Weber, in *Comprehensive Supramolecular Chemistry*, eds. R. Bishop, D. D. MacNicicol and F. Toda, Elsevier Science, Oxford, 1996, Vol. 6, p. 535.
10 G. R. Desiraju, I. C. Paul and D. Y. Curtin, *J. Am. Chem. Soc.*, 1977, **99**, 1594.
11 M. Tanaka, H. Matsui, J. Mizoguchi and S. Kashino, *Bull. Chem. Soc. Jpn.*, 1994, **67**, 1572.
12 M. Tanaka, H. Hayashi, S. Matsumoto, S. Kashino and K. Mogi, *Bull. Chem. Soc. Jpn.*, 1997, **70**, 329.
13 K. Shirai, M. Matsuoka and K. Fukunishi, *Dyes Pigm.*, 1999, **42**, 95.
14 J. Mizuguchi, *J. Phys. Chem. A*, 2000, **104**, 1817.
15 SAPI91: Hai-Fu Fan, Structure Analysis Programs with Intelligent Control, Rigaku Corporation, Tokyo, Japan, 1991.
16 SIR92: A. Altomare, M. C. Burla, M. Camalli, M. Cascarano, C. Giacovazzo, A. Guagliardi and G. Polidori, *J. Appl. Crystallogr.*, 1994, **27**, 435.
17 DIRDIF94: P. T. Beurskens, G. Admiraal, G. Beurskens, W. P. Bosman, R. de Gelder, R. Israel and J. M. M. Smits, The DIRDIF-94 program system, Technical Report of the Crystallography Laboratory, University of Nijmegen, The Netherlands, 1994.
18 teXsan: Crystal Structure Analysis Package, Molecular Structure Corporation, 1985 and 1992.